ISSN 1392-1207. MECHANIKA. Vol. 32, No. 2, 2026: 116–131

Research on Optimization Method of Vehicle Speed in Urban Road Conditions Based on Interval Analysis

Lingyun ZHU*, Haozhang SHI, Lei WANG***, Mingming QIU****, Han ZHAO*****
*School of Electrical Engineering and Intelligent Manufacturing, Anqing Normal University, Anqing, China,
E-mail: zhuly1028@126.com
**School of Mechanical Engineering, Hefei University of Technology, 230009 Hefei, China,
E-mail: 1442756147@qq.com
***Huawei Technologies Co., Ltd., 200121 Shanghai, China, E-mail: 1974727584@qq.com
****School of Mechanical Engineering, Hefei University of Technology, 230009 Hefei, China
E-mail: hfutqmm@hfut.edu.cn
*****School of Mechanical Engineering, Hefei University of Technology, 230009 Hefei, China,
E-mail: hanzhaoff@qq.com

https://doi.org/10.5755/j02.mech.41880

1. Introduction

In recent years, intelligent networked vehicles have received extensive attention from researchers worldwide as an effective solution for solving traffic congestion and reducing vehicle energy consumption. With the rapid development of technologies such as network communication and high-precision maps, intelligent networked vehicles are able to obtain an increasing amount of traffic information, which makes the vehicles still have room for improvement in reducing energy consumption. Especially in urban working conditions containing signal lights, vehicle driving is subject to the periodic intervention of signal lights, which are prone to rapid acceleration, rapid deceleration, and idling, resulting in poor vehicle traffic efficiency and low energy utilization. In an intelligent network environment, vehicles not only have the ability to obtain the current location information in real time, but also use vehicle-to-vehicle communication, vehicle-to-transportation infrastructure communication, and other technologies to realize multi-source information sharing [1]. Therefore, it remains a challenge to utilize the acquired vehicle and traffic information to enhance the vehicle economy in a smart grid environment.

Traffic information has an important influence on vehicle speed planning and plays an important role in reducing vehicle energy consumption. For urban working conditions, in order to make the vehicle travel speed meet road conditions while improving the economy, researchers at home and abroad have carried out much research. Vehicle speed planning in urban working conditions includes two aspects: traffic information processing and vehicle speed planning algorithms. In terms of traffic information processing, Asadi et al. designed a two-layer economical speed planning control strategy based on signal phase and time (SPaT) information, where the upper layer plans the speed range of the vehicle when passing on a green light based on regularized control logic, and the lower layer optimizes the speed based on model predictive control (MPC) [2]. Nie et al. used stratification to optimize vehicle speeds [3]. Jin et al. established an economical driving strategy that considered both the road speed limit and traffic light SPaT information [4].Xia et al. determined feasible passing speed intervals based on the roadway speed limit and traffic light SPaT information, and subsequently took their intersection as a way to obtain working condition information [5]. Homchaudhuri et al. proposed a discrete fuel economy control strategy, based on the traffic light SPaT information and the state information between neighbouring vehicles to derive the fleet of vehicles in the fleet of each vehicle to achieve the green light passing speed interval, as a constraint, the use of Fast-MPC to solve the whole fleet of optimal speed of the whole fleet of green-light passing [6]. Mandava et al. investigated an economic speed-planning strategy between two signals using conventional fuel vehicles [7]. Similarly, He et al. optimized the proportion of time in which vehicles move at a uniform speed or a uniform speed based on traffic light SPaT information based on the principle that vehicles only move at a uniform speed or a uniform speed between two signals [8]. Nunzio et al. established a speed pruning algorithm to compute the passable green light time range under the premise of meeting the road speed limit, used a graph search algorithm to search for the optimal "green window," and finally used a dynamic programming algorithm to solve the globally optimal speed trajectory with the goal of minimizing energy consumption [9]. It is not difficult to find that existing studies tend to consider only the single factor of signal lights when dealing with traffic information, or consider signal light SPaT information and simple road speed limits, while ignoring the traffic density information on the speed limit, which is the advantage of the strategy in this study.

To improve the efficiency of access and real-time speed planning, researchers have conducted extensive research on speed-planning algorithms. To improve the efficiency of vehicle traffic and solve the phenomenon of frequent rapid acceleration, rapid deceleration, and stop-start owing to irrational speed planning, Yugong et al. proposed an optimization strategy based on a genetic algorithm for hybrid vehicles to pass through continuous signalized intersections [10]. Xin Zhe et al. established a three-stage fuel-efficient driving pattern for a two-signal scenario with known multi-signal timing, and used the Floyd-Warshall shortest path algorithm to solve for the optimal speed under multiple signals [11]. To improve the real-time performance of the algorithm, Liao et al. performed simple speed planning based on signal light state information and body dynamic information and used a dynamic planning algorithm

to obtain the best reference speed profile for energy consumption [12]. Leng Jianghao et al. proposed an economical speed planning strategy combining dynamic programming algorithms and interior point method. The dynamic programming algorithm solves for the optimal green light cycle, and the optimal control problem is solved using the interior point method with the optimal green light cycle as the constraint [13]. Bo Zhang et al. designed a fast optimal speed planning strategy for predicting signal light information, obtaining the reference speed for passing the signal light ahead without stopping or braking based on the signal light status information, and using MPC to calculate the optimal driving speed of the vehicle in real time by combining with the goal of minimizing fuel consumption [14]. Liu et al. designed a two-tier speed planning method considering the communication distance, where the upper tier determines the passing speed interval, and the lower tier calculates the optimal energy-saving speed profile using a variable weight MPC [15]. Chen Hao et al. proposed a two-layer rolling distance domain speed optimization strategy considering signal light SPaT information, where the upper layer solves the global optimal speed trajectory based on Pontryagin's principle of minima, and the lower layer performs rolling optimization based on signal light information [16].

To summarize, the current speed planning considering traffic information under urban working conditions has achieved rich research results, but the existing research needs to be further improved in the following two aspects: 1. The current speed planning problem under urban road conditions focuses on the consideration of traffic signal phase information and road speed limit, but lacks the consideration of the speed limit of traffic conditions, and the adaptability of driving conditions is poor. 2. The speed planning algorithm used is difficult to balance global optimization with real-time performance. Therefore, in this paper, based on the consideration of traffic flow information and signal phase information, an economic speed planning method is designed based on the theory of interval analysis, which is applicable to the working conditions of urban roads. First, based on the traffic density information and signal phase information, metric automata and confidence interval theory are used to establish a traffic rule-based passing speed interval extraction method, and the permissible roadway-passing speed intervals under the current working conditions are obtained by simultaneously considering the signal SPaT information and traffic density information. Second, the MPC-DP speed planning method combining MPC and DP is established to calculate the optimal passing speed under the current working conditions to reduce the energy consumption of vehicles by using the Dynamic Programming (DP) algorithm in the predicted time domain controlled by the model prediction algorithm with the constraints of the acquired passing speed interval. Finally, the method proposed in this paper is comparatively analyzed through simulation and experimental validation to verify its effectiveness.

2. Vehicle Dynamics and Energy Consumption Modelling

In this paper, the intelligent network connected electric vehicle as the research object, in the vehicle network connection environment, the vehicle can obtain the signal

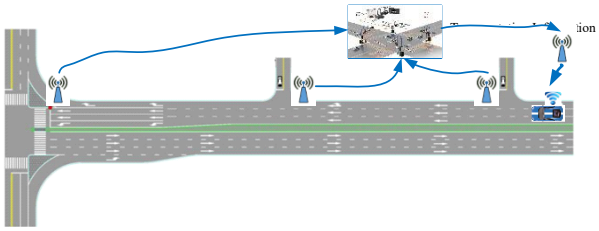

Fig.1 Vehicle traffic scenarios

light phase information and traffic density information under urban working conditions through V2I and V2V technology, the vehicle traffic scenario diagram, as shown in Fig. 1.

According to Newton's second law, the longitudinal dynamics of the vehicle is modeled as when the pure electric vehicle are driving unloaded on an urban road in a windless condition:

$$\frac{T_m \eta_t i_d}{r_w} = M_0 g \cos\theta \cdot f + \frac{C_d A_f v^2}{21.15} + \\ + M_0 g \sin\theta + \delta M_0 \frac{dv}{dt}, \tag{1}$$

where: T_m is the motor torque; η_t is the total efficiency of the transmission system; i_d is the reduction ratio of the gearbox; r_w is the wheel radius; M_0 is the mass of the whole vehicle equipment; g is the acceleration of gravity; f is the coefficient of rolling resistance; δ is the conversion factor of the rotating mass of the vehicle, $\delta > 1$; C_d is the wind resistance coefficient; A_f is the wind area; v is the vehicle driving speed; dv/dt is the acceleration of the vehicle driving; θ is the road slope, where $\theta = 0$, i.e., horizontal road, which is in line with the actual urban road.

The energy consumption of a pure electric vehicle is expressed using the integral of the output power of each battery cell over time:

$$E = \int_{T_0}^{T_0+\Delta T} P_b(t) dt, \tag{2}$$

where E denotes the pure electric vehicle energy consumption shared by each battery cell at time ΔT.

The drive motor is a permanent magnet synchronous motor, and the motor efficiency is obtained by interpolating the table:

$$\eta_m = f_1(n_m, T_m), \tag{3}$$

$$n_m = \frac{60v}{2\pi r_w} \cdot i_d, \tag{4}$$

where η_m denotes the motor efficiency; n_m denotes the motor speed; and T_m denotes the motor output torque.

The motor power is:

$$P_m = \begin{cases} \dfrac{T_m n_m}{9550\eta_m}, & T_m \geq 0 \\ \dfrac{T_m n_m \eta_m}{9550}, & T_m < 0 \end{cases}, \tag{5}$$

where, when $T_m \geq 0$, the motor drives the vehicle forward; $T_m < 0$, the motor is in the feedback braking dynamic.

The power battery pack used in this paper consisted of multiple battery monomers connected in series and parallel. The changes in the internal resistance of each battery cell during charging and discharging are shown in Fig. 2. The battery model uses an equivalent circuit model, and the battery SOC changes during charging and discharging, as follows:

$$\frac{dSOC}{dt} = \begin{cases} \dfrac{U_0 - \sqrt{U_0^2 - 4P_bR_d}}{2R_dQ_{bat}} \\ \dfrac{\sqrt{U_0^2 - 4P_bR_c} - U_0}{2R_cQ_{bat}} \end{cases}, \tag{6}$$

where $dSOC/dt$ is the rate of change of battery SOC with time; Q_{bat} is the battery capacity; U_0 is the open-circuit voltage of the battery in V; R_d and R_c denote the battery discharging and charging resistances in Ω, respectively; I_d and I_c denote the battery discharging and charging currents in A, respectively.

This paper establishes a wheel-mileage energy consumption model. Associative Eqs. (1), (3), (4) and (5) obtain the total output power P_m of the drive motor and the output power P_b of the battery monomer as:

$$P_m = \begin{cases} \left(M_0gf + \dfrac{C_dA_fv^2}{21.15} + \delta M_0\dfrac{dv}{dt}\right)\cdot \\ \dfrac{30v}{\pi\eta_t}\cdot\dfrac{1}{9550\eta_m} \quad \text{Electric motor drive;} \\ \left(M_0gf + \dfrac{C_dA_fv^2}{21.15} + \delta M_0\dfrac{dv}{dt}\right)\cdot \\ \dfrac{30v}{\pi\eta_t}\cdot\dfrac{\eta_m}{9550} \quad \text{Motor feed-back braking.} \end{cases} \tag{7}$$

$$P_b = \frac{1}{N_{total}}\cdot\frac{P_m}{\eta_b}, \tag{8}$$

where N_{total} is the total number of battery cells.

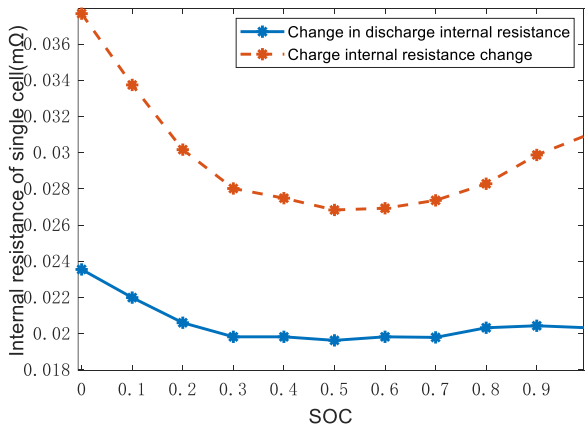

Fig. 2 Battery charge and discharge internal resistance change

Associating Eqs. (2), (6), (7), and (8) yields that the battery cell power consumption in ΔT time is:

$$\Delta SOC = \begin{cases} \int_{T_0}^{T_0+\Delta T} \dfrac{U_0 - \sqrt{U_0^2 - 4P_bR_d}}{2R_dQ_{bat}}dt \\ \text{Battery-discharging,} \\ \int_{T_0}^{T_0+\Delta T} \dfrac{\sqrt{U_0^2 - 4P_bR_c} - U_0}{2R_cQ_{bat}}dt \\ \text{Battery-charging.} \end{cases} \tag{9}$$

3. Passing Speed Interval Extraction Method Based on Road Passing Rules

Traffic signals are an important factor affecting vehicle traffic in urban road conditions, and their signal reception distance has a significant impact on the accuracy and efficiency of condition prediction [17-18]. Therefore, in this paper, considering the reception distance of signalized information, a segmented continuous signalized intersection passing speed interval extraction method is designed by using the traffic density information, and the calculation flow is shown in Fig. 3.

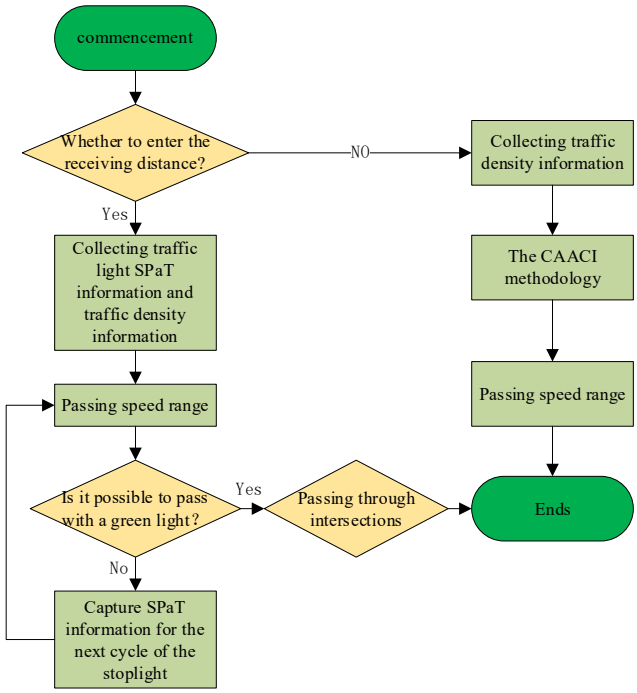

Fig. 3 Passing speed zone extraction process

3.1 Traffic signal phase information model

To simplify the passing speed interval extraction problem, the following assumptions are made regarding the signalized SPaT information:

1. The traffic signal timing is fixed, that is, once a vehicle obtains the phase information of the traffic light, the phase timing information remains unchanged.

2. The obtained phase information is accurate and reliable without any interference.

3. Treating yellow light as red for safe passage.

4. Vehicles can pass through an intersection at the time of signal switching.

Define the initial time as $t = 0$. If the signal light at the m-th intersection is green, the timing information obtained at the initial moment for the m-th intersection is denoted as $T_g^m(0)$; if it is red, the timing information is denoted as $T_r^m(0)$. At time t, the remaining timing information when the signal light at the m-th intersection is green is denoted as $T_g^m(t)$, and when it is red, it is denoted as $T_r^m(t)$, where $m = 1, 2, 3, \ldots K$, and K is the total number of signalized intersections. Additionally, the total green light timing and total red light timing for the m-th intersection are denoted as ΔT_g^m and ΔT_r^m, respectively.

When $t < \Delta T_g^m(0)$ or $t < \Delta T_r^m(0)$, it indicates that the current time has not exceeded the signal timing duration. If the signal at the m-th intersection is green, then:

$$T_g^m(t) = T_g^m(0) - t. \tag{10}$$

If the signal light at the m-th intersection is red, then:

$$T_r^m(t) = T_r^m(0) - t. \tag{11}$$

When $t \geq T_r^m(0)$, it indicates that the current time has exceeded the signal light's timing duration. If the signal light at the m-th intersection is green, then:

$$t_{wg} = \left(t - T_g^m(0)\right)\%\left(\Delta T_g^m + \Delta T_r^m\right). \tag{12}$$

At this point, if t_{wg} is less than the total red light duration ΔT_r^m, then:

$$T_r^m(t) = \Delta T_r^m - t_{wg}. \tag{13}$$

If t_{wg} is greater than the total red light duration ΔT_r^m and less than the total signal duration $\Delta T_g^m + \Delta T_r^m$, then:

$$T_g^m(t) = \Delta T_g^m + \Delta T_r^m - t_{wg}. \tag{14}$$

If the signal at the m-th intersection is red, then:

$$t_{wr} = \left(t - T_r^m(0)\right)\%\left(\Delta T_g^m + \Delta T_r^m\right). \tag{15}$$

At this point, if t_{wr} is less than the total green light duration ΔT_g^m, then:

$$T_g^m(t) = \Delta T_g^m - t_{wr}. \tag{16}$$

If t_{wg} is greater than the total red light duration ΔT_r^m and less than the total signal duration $\Delta T_g^m + \Delta T_r^m$, then:

$$T_r^m(t) = \Delta T_g^m + \Delta T_r^m - t_{wr}. \tag{17}$$

Let the reception distance of the traffic light signal be d. Considering that the vehicle receiving the signal information and traffic density information needs enough processing time and speed planning and control time, the reception distance d is:

$$d = \left(\Delta T_g^m + \Delta T_r^m\right) * v_l, \tag{18}$$

where $(\Delta T_g^m + \Delta T_r^m)$ is the signal period; v_l is the recommended passing speed of urban roads, and $v_l = 40$ km/h is taken in this paper.

3.2. Establishment of rules of the road

In this paper, based on the theory of cellular automata (CA), we introduce the vehicle random initialization rule, Gipps safety distance rule, and random lane-changing rule to establish the road access rule model.

Considering a circular road with length and number of lanes as an object, each lane is partitioned into tuples with spacing according to the length of the vehicle, and the total number of tuples per lane is G:

$$G = \frac{S}{\Delta s}. \tag{19}$$

The state equation for the i-th vehicle in the lane is:

$$\begin{cases} v_i(x,y) \in [0, V_{max}] \\ s_i(x,y) \\ x \in [1,2,\ldots,G] \\ y \in [1,2,\ldots,n] \end{cases}, \tag{20}$$

where $v_i(x, y)$ denotes the speed of the i-th vehicle; $s_i(x, y)$ denotes the location of the i-th vehicle; x denotes the number of cellulars; and y denotes the number of lanes.

Then the total number of vehicles entering the roadway Q:

$$Q = \frac{c_s S}{1000}. \tag{21}$$

where c_s is the traffic density in vehicles/km.

On this basis, a double random initialization algorithm is used to initialize the vehicle position and speed, and the specific process is shown in Fig. 4.

After the initialization is complete, the vehicle is iteratively updated according to the period Δt, following the road access rules. The road passing rules are as follows

1. Safety Distance Rules for Front and Rear Vehicles

When the front car emergency braking, in order to avoid rear-end collision, this paper adopts the Gipps safety distance rule to correct the safety distance between the front and rear cars. Specifically, as follows:

$$gap_i = s_{i+1}(x,y,t) - s_i(x,y,t) - l, \tag{22}$$

$$gap_{safe,i} = v_i(x,y,t)\tau + \frac{v_i(x,y,t)^2}{2a_{max,i}} - \frac{v_{i+1}(x,y,t)^2}{2a_{max,i+1}}, \tag{23}$$

where gap_i denotes the actual distance between the i-th vehicle and the vehicle in front of it; $gap_{safe,i}$ is the distance

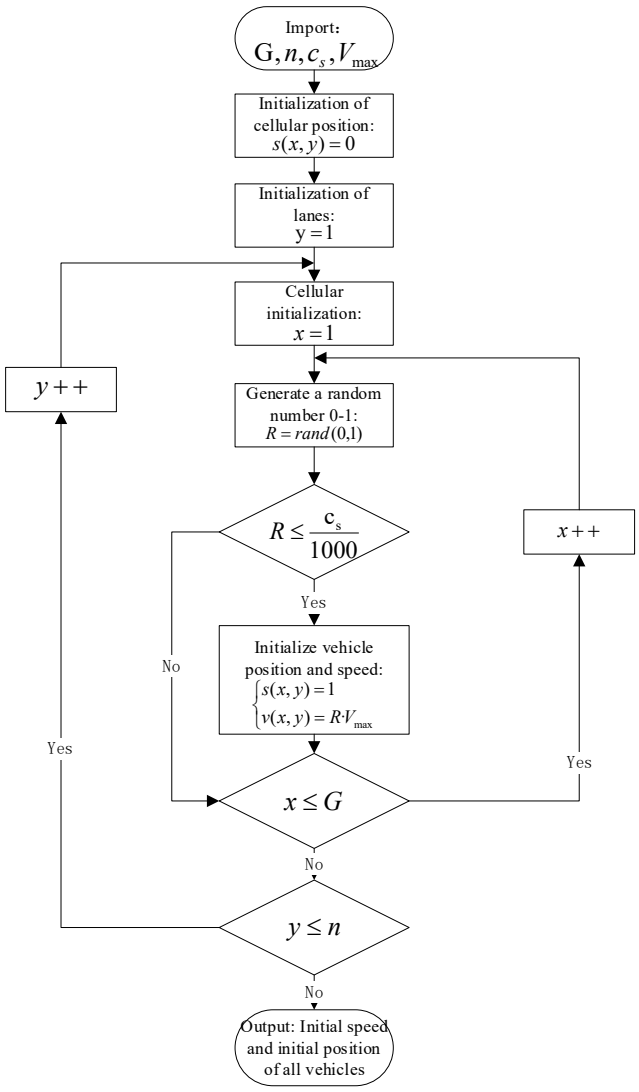

Fig. 4 Double random initialization process

calculated according to Gipps' safe distance rule; $s_i(x, y, t)$ and $s_{i+1}(x, y, t)$ are the locations of the i-th vehicle and the vehicle directly in front of it at the moment of t, respectively; l is the vehicle length; $v_i(x, y, t)$ and $v_{i+1}(x, y, t)$ are the speeds of the i-th vehicle and the vehicle directly in front of it at the moment of t, respectively; τ is the driver reaction time; $a_{max,i}$ and $a_{max,i+1}$ are the maximum deceleration of the i-th vehicle and the vehicle directly in front, respectively.

$R \le \frac{c_s}{1000}$.

2. Acceleration rules

When the distance between the i-th vehicle and the vehicle in front is greater than the safe distance, the vehicle accelerates, the vehicle's speed does not exceed the maximum speed, and the acceleration distance does not exceed the actual distance between the vehicles, the rules are as follows:

$$\begin{cases} gap_i > gap_{safe,i} \\ v_i(x, y, t+\Delta t) = min\left(\begin{matrix} v_i(x, y, t) + \\ +a_{acc}\Delta t, V_{max}, \frac{gap_i}{\Delta t} \end{matrix} \right) \end{cases}, \quad (24)$$

where, $v_i(x, y, t+\Delta t)$ is the velocity of the i-th vehicle at the moment $t+\Delta t$ and a_{acc} is the standard acceleration of the vehicle.

3. Deceleration rules

When the distance between vehicle i and the vehicle in front is less than the safe distance, the vehicle decelerates by no more than the actual distance between vehicles:

$$\begin{cases} gap_i < gap_{safe,i} \\ v_i(x, y, t+\Delta t) = min\left(\begin{matrix} v_i(x, y, t) - \\ -a_{acc}\Delta t, \frac{gap_i}{\Delta t} \end{matrix} \right) \end{cases}. \quad (25)$$

4. Randomized slowing rules

Considering the problem of vehicle deceleration caused by uncertainty in the driving process, this paper introduces a stochastic slowdown rule as follows:

$$v_i(x, y, t+\Delta t) = max\left(\begin{matrix} v_i(x, y, t) - \\ -a_{dec} \cdot \Delta t, 0 \end{matrix} \right). \quad (26)$$

5. Position update rules

The rules for updating the position of a vehicle while it is in motion are as follows:

$$\begin{aligned} s_i(x, y, t+\Delta t) &= s_i(x, y, t) + \\ &+ v_i(x, y, t+\Delta t) \cdot \Delta t. \end{aligned} \quad (27)$$

6. Switching rules

Vehicle lane change includes two scenarios: lane change to the left and lane change to the right. When the vehicle satisfies both scenarios, the right lane change is preferred.

a. Left lane change rule

When changing lanes to the left, the vehicle accelerates, and the acceleration distance should be greater than the actual distance between the vehicle and the downstream section of the left lane, the first position $s_i(x-1, y+1, t)$ and the second position $s_i(x-2, y+1, t)$ are free of vehicles, the left lane $s_i(x, y+1, t)$ is free of vehicles, and all the positions between the upstream section of the left lane and the front vehicle of the current lane $s_i(x+gap_i, y+1, t)$ are free of vehicles. All positions $s_i(x+gap_i, y+1, t)$:

$$\begin{cases} v_i(x, y, t) > \frac{gap_i}{\Delta t} \\ s_i(x-1, y+1, t) = 0 \\ s_i(x-2, y+1, t) = 0 \\ s_i(x, y+1, t) = 0 \\ s_i(x+gap_i, y+1, t) = 0 \end{cases}. \quad (28)$$

b. Right lane change rule

Since the right lane change is a deceleration change, it is only necessary to satisfy that there are no cars in the right lane $s_i(x, y+1, t)$, no cars in the first position and the second position downstream of the right lane, and no cars in the first position and the second position upstream of the right lane, i.e:

$$\begin{cases} s_i(x, y-1, t)=0 \\ s_i(x-1, y-1, t)=0 \\ s_i(x-2, y-1, t)=0 \\ s_i(x+1, y-1, t)=0 \\ s_i(x+2, y-1, t)=0 \end{cases}. \tag{29}$$

7. Vehicle re-entry rules

In order to ensure that the current traffic density on the road does not change, when the vehicle's position $s_i(x, y, t)$ exceeds the total number of tuples, at this point it reverts back to the initial position of the road segment.

3.3. Confidence interval-based extraction of passing speed intervals

The speed interval for passing through a signalized roadway is determined by a combination of the vehicle's distance from the signal, signal timing, and traffic density information. Depending on whether the vehicle's distance from the traffic light ahead enters the receiving distance, there are two scenarios:

1. Not within receiving distance

When it has not entered the receiving distance, at this time the vehicle only considers the traffic density information. By iterating through the road access rules, when the iteration ends, the distribution of speed points appearing in each tuple on the current road can be obtained, i.e., the distribution of vehicle speeds under the current traffic density. By further processing the obtained speed points, a centralized and reasonable speed interval is obtained.

Confidence interval refers to the overall parameter estimation interval constructed from the sample total, which indicates the degree to which the true value of this parameter has a certain probability to fall around the measurement result. This paper adopts the theory of confidence intervals, the speed point distribution obtained earlier as a sample total, to solve the 95% confidence level to meet the confidence interval, that is, the current traffic density allows a reasonable passing speed interval. The specific steps are as follows:

Step 1: Calculate the overall mean $\bar{X}$ and standard deviation σ of the sample of velocity points.

Step 2: Calculate the value of α based on the 95% confidence level:

$$\alpha = 1 - 0.95 = 0.05 . \tag{30}$$

Step 3: Find the value of $z_{\alpha/2}$ from the standard normal distribution table.

Step 4: A confidence interval that satisfies the 95% confidence level is derived, i.e., the passing speed interval H:

$$H = \left(\bar{X} - z_{\alpha/2} \frac{\sigma}{\sqrt{n}}, \bar{X} + z_{\alpha/2} \frac{\sigma}{\sqrt{n}} \right). \tag{31}$$

2. Getting within receiving distance

Access to the reception distance range, need to take into account both traffic density information and signal information.

Firstly, the passing speed interval under the current working condition is extracted according to the road vehicle density information, and the extraction process is the same as that for the case of not entering the receiving distance range, and the passing speed interval under the current traffic density, $H_{s,c}^t$, is recorded as:

$$H_{s,c}^t = \left[v_{min,c}^t, v_{max,c}^t \right]. \tag{32}$$

Secondly, according to the traffic signal information, the passing speed interval is extracted in accordance with the principle of all-green-light passing and reduction of high energy-consuming working conditions such as vehicle starting, idling and stopping. Let J^m be the m-th signal cycle number, d_t^m is the distance between the vehicle at this time and the m-th signal ahead, as a scalar. This time is divided into two cases:

a. When $J^m = 1$, i.e., the current received beacon cycle is the first cycle.

When the received signal is green, the upper and lower speed limits are shown in Fig. 5.

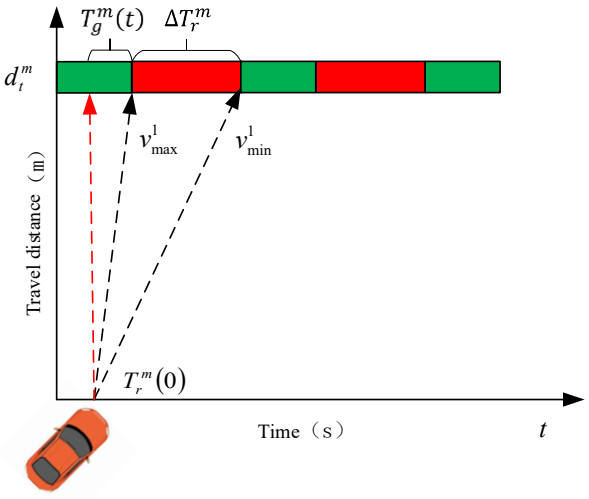

Fig. 5 Feasible velocity intervals for the first cycle (during green phase)

The upper speed limit v_{max}^1:

$$v_{max}^1 = \frac{d_t^m}{T_g^m(t)} . \tag{33}$$

The lower speed limit v_{min}^1:

$$v_{min}^1 = \frac{d_t^m}{T_g^m(t) + \Delta T_r^m} . \tag{34}$$

When the received signal is red, the upper and lower speed limits are shown in Fig. 6.

The upper speed limit v_{max}^1:

$$v_{max}^1 = \frac{d_t^m}{T_r^m(t)} . \tag{35}$$

The lower speed limit v_{min}^1:

$$v_{min}^1 = \frac{d_t^m}{T_r^m(t) + \Delta T_g^m} . \tag{36}$$

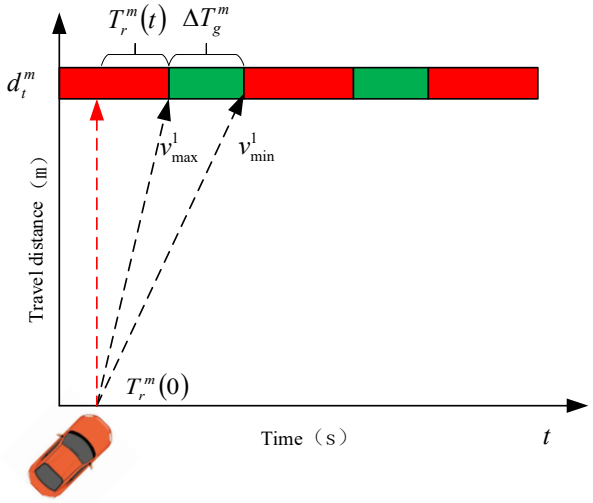

Fig. 6 Feasible velocity intervals for the first cycle (during red phase)

As a result, the passing speed interval $H_{s,l}^t$ obtained from the traffic signal information is:

$$H_{s,l}^t = \left[v_{min}^1, v_{max}^1 \right]. \tag{37}$$

At this time, the roadway passing speed interval is determined based on the intersection of $H_{s,c}^t$ and $H_{s,l}^t$, as shown in Fig. 7. Among them, cases 4 and 5 have no intersection, and the new passing speed interval needs to be recalculated at this time, and case 6 is the case in which $H_{s,c}^t$ belongs to $H_{s,l}^t$, and $H_{s,c}^t$ doesn't need to be recalculated, and it is enough to keep it unchanged, and then it needs to be adjusted to $H_{s,l}^t$: change the cycle of the vehicle when it passes through the red traffic light, i.e., adjust J^m.

b. When $J^m > 1$, it is an indication that the vehicle is unable to obtain the appropriate passing speed interval during the first traffic light cycle.

When the received signal is green, the upper and lower speed limits are shown in Fig. 8.

The upper speed limit $v_{max}^{J^m}$

$$v_{max}^{J^m} = v_{min}^{J^m-1}, \tag{38}$$

where $v_{min}^{J^m-1}$ is the lower limit of velocity determined in the previous cycle.

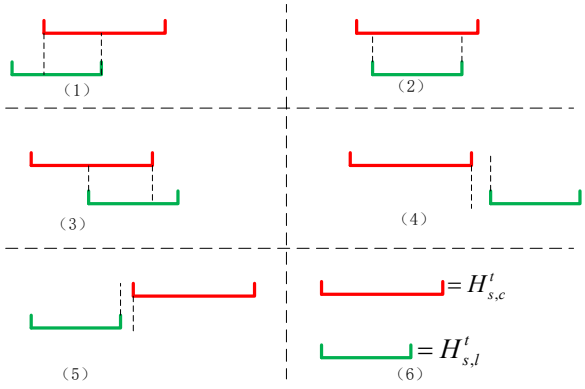

Fig. 7 Plot of the distribution of the two speed intervals

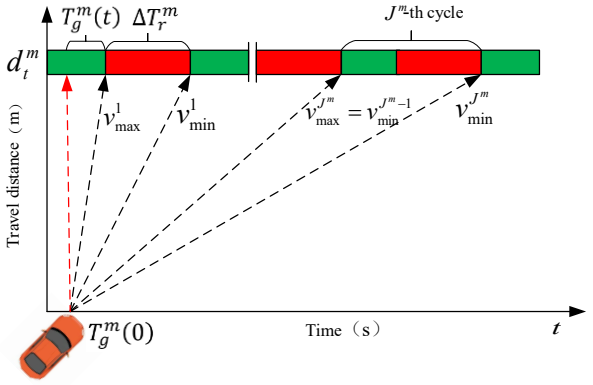

Fig. 8 J^m-th cycle feasible velocity interval (during green phase)

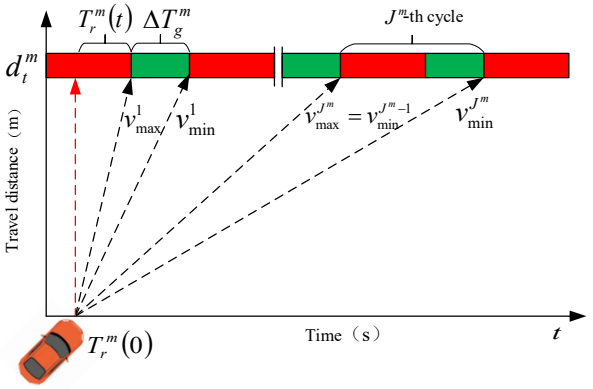

Fig. 9 J^m-th cycle feasible velocity interval (during red phase)

Lower speed limit $v_{min}^{J^m}$

$$v_{min}^{J^m} = \frac{d_t^m}{T_g^m(t) + J^m \Delta T_r^m + \left(J^m - 1\right)\Delta T_g^m}. \tag{39}$$

When the received signal is red, the upper and lower speed limits are shown in Fig. 9.

The upper speed limit $v_{max}^{J^m}$

$$v_{max}^{J^m} = v_{min}^{J^m-1}, \tag{40}$$

where $v_{min}^{J^m-1}$ is the lower limit of velocity determined in the previous cycle.

Lower speed limit $v_{min}^{J^m}$

$$v_{min}^{J^m} = \frac{d_t^m}{T_r^m(t) + J^m \Delta T_g^m + \left(J^m - 1\right)\Delta T_r^m}. \tag{41}$$

The passing speed interval $H_{s,l}^t$ determined from the signalized information is:

$$H_{s,l}^t = \left[v_{min}^{J^m}, v_{max}^{J^m} \right]. \tag{42}$$

If $H_{s,l}^t$ and $H_{s,c}^t$ still do not intersect, continue to calculate $H_{s,l}^t$ for the next traffic light cycle, i.e., $J^m = J^m + 1$ and so on until $H_{s,l}^t$ and $H_{s,c}^t$ intersect.

In summary, the passing speed interval $H_{s,c,l}^t$ that satisfies both traffic density information and signalization information is:

$$H_{s,c,l}^t = H_{s,l}^t \cap H_{s,c}^t . \tag{43}$$

$H_{s,c,l}^t$ is based on the realization of all-green-light passing, and fully considers the traffic flow limitations on passing speeds.

4. Vehicle Speed Planning for Economy

4.1. Vehicle speed planning modeling

4.1.1. Objective function

Establish the optimization objective function with the goal of minimizing vehicle energy consumption:

$$min\, J = \int f_{eco}(t)dt , \tag{44}$$

where $f_{eco}(t)$ is the vehicle energy consumption rate, which is related to vehicle parameters.

Combining Eqs. (9) and (44) yields the objective function for the discharged and charged states of the battery:

Discharge state

$$min\, J = \int \left[\frac{U_0 - \sqrt{U_0^2 - 4P_b R_d}}{2 \cdot R_d Q_{bat}} \right] dt . \tag{45}$$

Charge state

$$min\, J = \int \left[\frac{\sqrt{U_0^2 - 4P_b R_c} - U_0}{2 R_c Q_{bat}} \right] dt . \tag{46}$$

4.1.2. Boundary conditions and constraints

The vehicle departs from position s_0 at moment t_0 with speed v_0 and arrives at s_k at moment t_k with speed v_k, so the optimization boundary condition is:

$$\begin{cases} s(t_0) = s_0 , v(t_0) = v_0 \\ s(t_k) = s_k , v(t_k) = v_k \end{cases} . \tag{47}$$

The constraints for optimization include two parts: 1. Structural constraints on the vehicle's own parameters, including the output torque and output power of the engine or motor, the limiting speed and limiting acceleration, and the maximum current of the battery, etc., which are related to the vehicle model. 2. Non-structural constraints determined by the road traffic environment, including road gradient, road speed limit, road curve curvature, traffic flow information and traffic light phase information, etc., which are time-varying. Therefore, in this paper, both structural and non-structural constraints of the vehicle are considered, which can maximize the economy of the vehicle.

The structural constraints are:

$$\begin{cases} SOC_{min} \le SOC \le SOC_{max} \\ T_{m,min} \le T_m \le T_{m,max} \\ P_{m,min} \le P_m \le P_{m,max} \\ I_{min} \le I \le I_{max} \\ a_{min} \le a \le a_{max} \end{cases} . \tag{48}$$

Among them, *SOK* represents the charging state of the battery, SOK_{min} and SOK_{max} are the minimum and maximum values of the charging state of the battery, respectively; T_m represents the output torque of the motor, $T_{m,min}$ and $T_{m,max}$ represent the minimum and maximum output torque of the motor, respectively; P_m denotes the motor output power, $P_{m,min}$ and $P_{m,max}$ denote the minimum and maximum motor output power, respectively; I denotes the battery discharge current, I_{min} and I_{max} denote the minimum and maximum battery discharge current, respectively; and a denotes the vehicle acceleration, a_{min} and a_{max} denote the minimum and maximum vehicle acceleration, respectively.

Non-structural constraints are:

$$v \in H_{s,c,l}^t \text{ Continuous signal} , \tag{49}$$

where $H_{s,c,l}^t$ is the roadway speed interval terminated from traffic signal and traffic density information.

4.1.3. Vehicle speed planning model

Eqs.: (44), (47), (48), and (49) lead to a model of the economic vehicle speed planning problem:

$$min\, J = \int f_{eco}(t)dt . \tag{50}$$

The constraints are:

$$\begin{cases} SOC_{min} \le SOC \le SOC_{max} \\ T_{e,min} \le T_e \le T_{e,max} \\ P_{e,min} \le P_e \le P_{e,max} \\ I_{min} \le I \le I_{max} \\ a_{min} \le a \le a_{max} \\ v \in H_{s,c,l}^t , \text{Signal light intersections} \\ s(t_0) = s_0 , v(t_0) = v_0 \\ s(t_k) = s_k , v(t_k) = v_k \end{cases} . \tag{51}$$

4.2. Real-time vehicle speed planning based on MPC-DP algorithm

MPC is a local optimal solution method that optimizes only the control sequences in the prediction domain of the system and updates the optimal control outputs in real time by optimizing them on a rolling basis [19]. DP is a global optimization method, and the global optimization capability of MPC can be improved by using DP solution in the prediction domain [20]. Let the prediction time domain of MPC be N_p, and the control time domain be N_c, the displacement s and velocity v of the vehicle are selected as the state variables, i.e., $\boldsymbol{x} = [s \;\; v]^T$, and the total output torque of

the vehicle, T_z is the control variable, i.e., $\boldsymbol{u} = T_z$, then the state space of the vehicle's longitudinal motion is:

$$\begin{cases} \dot{s} = v \\ \dot{v} = \dfrac{T_z}{M_0 r_w} - \dfrac{F_r}{M_0} \end{cases}, \tag{52}$$

where M_0 denotes the mass of the whole vehicle, r_w denotes the radius of the tire, g denotes the acceleration of gravity, f denotes the coefficient of friction, C_d, denotes the coefficient of wind resistance, A_f denotes the area of the windward side; and F_r denotes the driving resistance:

$$F_r = M_0 g\left(f\cos\theta + \sin\theta\right) + \frac{C_d A_f v^2}{21.5}. \tag{53}$$

Setting T_s as the sampling period and discretizing Eqs. (52) and (53), the model can be predicted as:

$$\begin{cases} x(k+1) = A_k x(k) + B_k u(k) + D_k \varphi(k) \\ A_k = \begin{bmatrix} 0 & T_s \\ 0 & 0 \end{bmatrix} \\ B_k = \begin{bmatrix} 0 \\ \dfrac{T_s}{M_0 r_w} \end{bmatrix} \\ D_k = 1 \\ \varphi = -\dfrac{T_s F_r}{M_0} \end{cases}, \tag{54}$$

where k is the current sampling moment; k+1 is the next sampling moment.

Next, the feasible state space of vehicle speeds in the predicted time domain is discretized in the time domain according to the passing speed interval $H^t_{s,c,l}$. The discretization step is set to Δv and the distribution of speed points after discretization is shown below:

$$\begin{bmatrix} H^t_{s,c,l,min}, H^t_{s,c,l,min} + \Delta v, \\ H^t_{s,c,l,min} + 2\Delta v, \ldots, H^t_{s,c,l,max} \end{bmatrix}, \tag{55}$$

where $H^t_{s,c,min}$ and $H^t_{s,c,max}$ are the lower and upper limits of $H^t_{s,c}$; $H^t_{s,c,l,min}$ and $H^t_{s,c,l,max}$ are the lower and upper limits of $H^t_{s,c,l}$.

Then the Dynamic Programming (DP) algorithm is used to solve the objective function in the prediction time domain N_p to ensure the global optimization in the prediction time domain N_p, so as to obtain the optimal control variable sequence. The specific solution process is as follows:

Taking the prediction time domain N_p as the planning time and dividing it into N phases, Eq. (44) is discretized in the time domain, and the discretization interval is Δt, so the objective function can be obtained:

$$\min J = \sum_{k=0}^{N-1} \left[f_{eco}\left(x(k), u(k)\right) \right] \cdot \Delta t. \tag{56}$$

The N subproblems are then solved inversely.

Step N–1

$$J^*_{N-1}\left(x(N-1)\right) = \\ = \min \begin{bmatrix} f_{eco}\left(x(N-1), u(N-1)\right) \cdot \Delta t + \\ + W\left(x(N)\right) \end{bmatrix}. \tag{57}$$

Step k, $0 \le k < N$–1

$$J^*_k\left(x(k)\right) = \min \begin{bmatrix} f_{eco}\left(x(k), u(k)\right) \Delta t + \\ + J^*_{k+1}\left(x(k+1)\right) \end{bmatrix}. \tag{58}$$

Here $W(x(N))$ is the objective function of the terminal substage, $J^*_k(x(k))$ denotes the optimal value function from the k-th stage to the terminal.

The optimal output torque sequence in the whole prediction time domain N_p can be obtained after solving by dynamic programming. Subsequently, the first element of the optimal output torque sequence is inputted into the system, and after a control time domain N_c, the vehicle speed at the (k+N_c)-th moment is calculated, and the cycle rolling optimization is carried out to realize the MPC-based full roadway speed planning.

5. Simulation and Experimental Verification Analysis

5.1. Simulation analysis

In this section, the effectiveness of speed planning based on interval analysis theory under urban road conditions is verified through simulation and experiment, and the simulation model is shown in Fig. 10. The distance traveled, speed, acceleration, motor output torque, battery SOC consumption and motor operating point are used as evaluation indexes to compare the speed planning strategy with the traditional speed planning strategy that only considers signal lights under the same traffic condition. Simulation conditions: the total length of the continuous signalized intersection is 1500 m, there are 5 signals, and the phase information of each signal is shown in Table 1. the speed limit of the road is 72 km/h, and the minimum speed to ensure the efficiency of the traffic is 14km/h. The initial SOC of the simulation is set to 0.8, and the initial speed is 50 km/h. The specific parameters of the vehicle are shown in Table 2, and the other parameters of the simulation are shown in Table 3

The results in Fig. 11 show that the speed planning strategy proposed in this paper realizes all-green light passing. Fig. 12 shows the energy optimal vehicle speed, the vehicle speed changes gently without large fluctuations, which is conducive to reducing energy consumption. Fig. 13 shows the energy optimal acceleration, after increasing the passing speed interval constraint, the number of sharp acceleration and sharp deceleration of the vehicle are significantly reduced. Fig. 14 shows the motor operation work point, mostly distributed in the middle and low-speed high-efficiency intervals, which is due to the consideration of traffic density information, with a certain degree of predictability, to reduce the wide range of speed fluctuations.

In order to further prove the superiority of the proposed strategy in this paper, the MPC vehicle speed

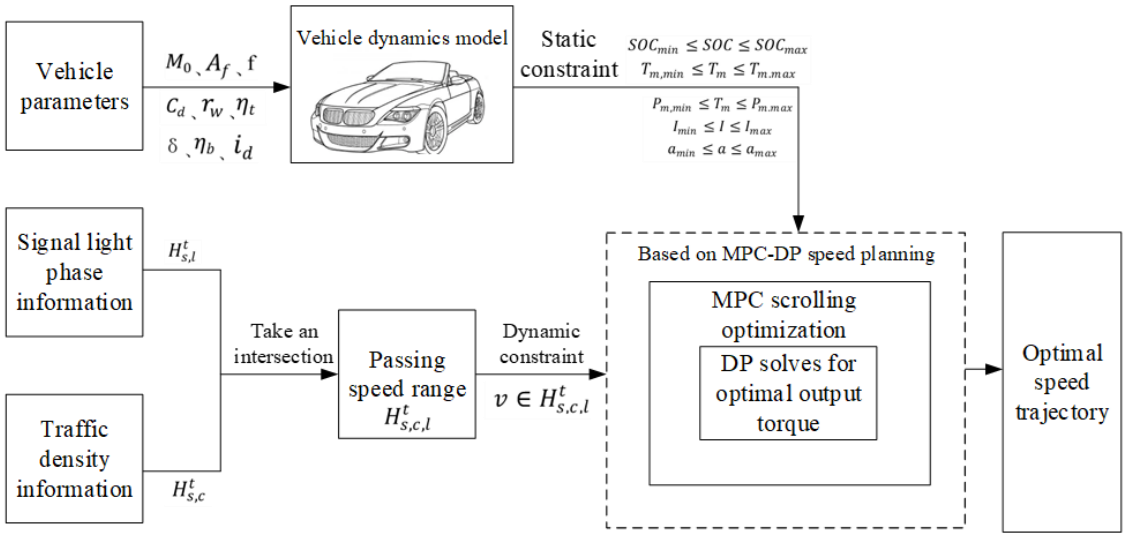

Fig. 10 Vehicle speed simulation model structure

Table1

Five signal phasing information

Junction ids	Junction location, m	Red light timing info, s	Green light timing info, s
1	200	30	40
2	600	30	40
3	900	30	40
4	1300	30	40
5	1500	20	20

Table2

Pure electric vehicle parameters

Parameter names	Symbols, units	Parameter values
Total vehicle mass	M_0, kg	2100
Frontal windward area	A_f, m^2	2.56
Rolling resistance factor	f	0.01
Wind resistance factor	C_d	0.36
Tire radius	r_w, m	0.353
Rotational mass conversion factor	δ	1.332
Total driveline efficiency	η_t	0.9
Air density	ρ, N×s^2×m^{-4}	1.2258
Gravitational acceleration	g	9.8
Battery conversion efficiency	η_b	0.92
Reduction ratio	i_d	7.8812

planning strategy [14, 21], which only considers the phase information of signals, is used as a reference for comparative simulation, and the arrival times of the two strategies are guaranteed to be the same during the simulation. Figs. 15, 16, 17, 18 and 19 show the comparison results of the two strategies corresponding to vehicle displacement, speed, acceleration, SOC consumption and motor operating point, respectively.

Table3

Simulation parameters of the rule-like method

Parameter values	Symbols, units	Numerical
Metameric length	Δs, m	5
Road length	S, m	200
Update time cycle	Δt, s	1
Vehicle length	l, m	5
Maximum vehicle speed	V_{max}, km/h	120
Maximum deceleration	$a_{max,i}$, m/s^2	6
Standard accelerations	a_{acc}, m/s^2	4
Stochastic moderated probability	p_{slow}	0.2
Randomized slowdown reduction	a_{dec}, m/s^2	2

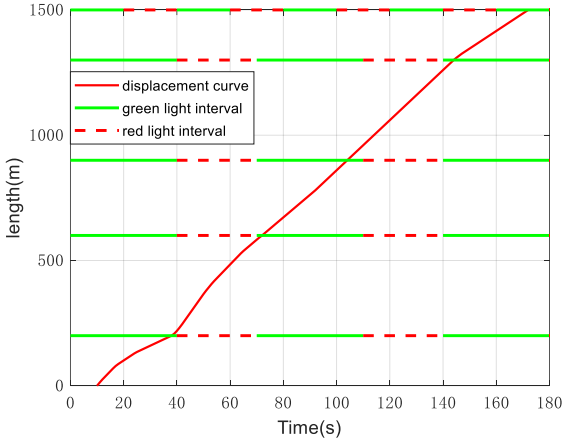

Fig. 11 Displacement curve for all-green light passing

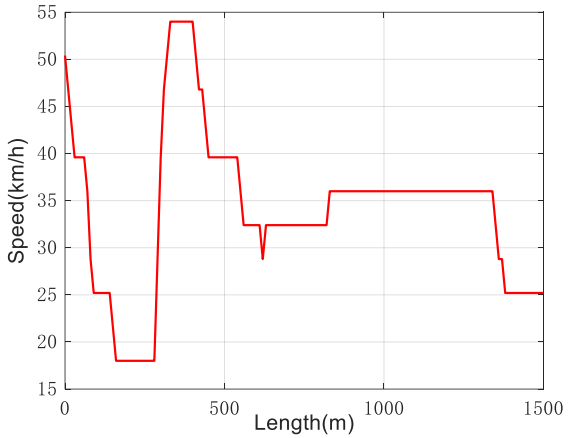

Fig. 12 Vehicle speed trajectory

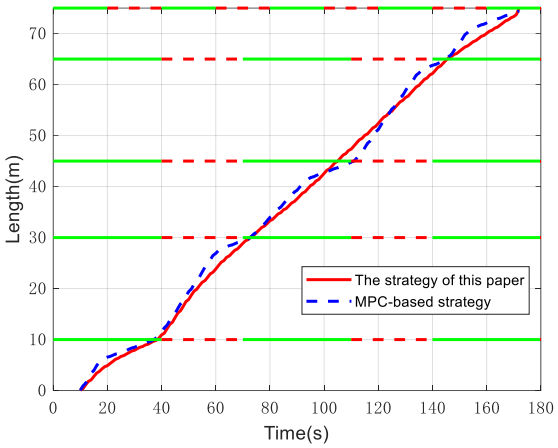

Fig. 3 Comparison of pass-through displacement curves

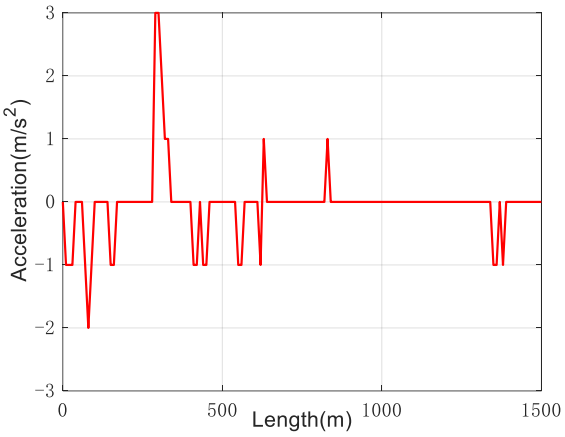

Fig. 1 Acceleration trajectory

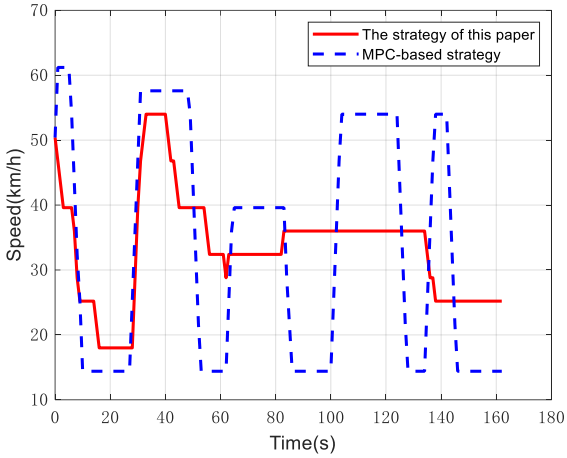

Fig. 4 Vehicle speed trajectory comparison

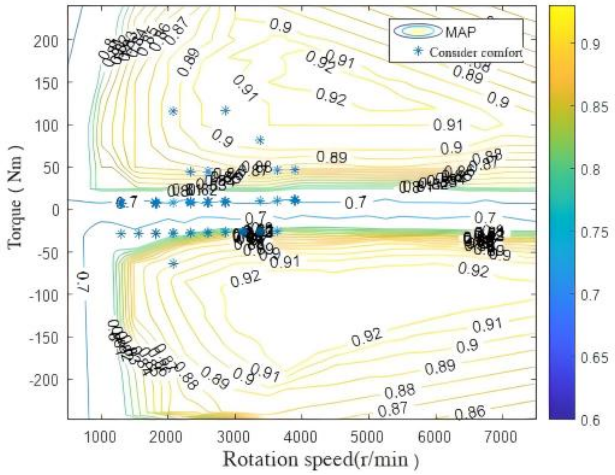

Fig. 2 Motor operating point

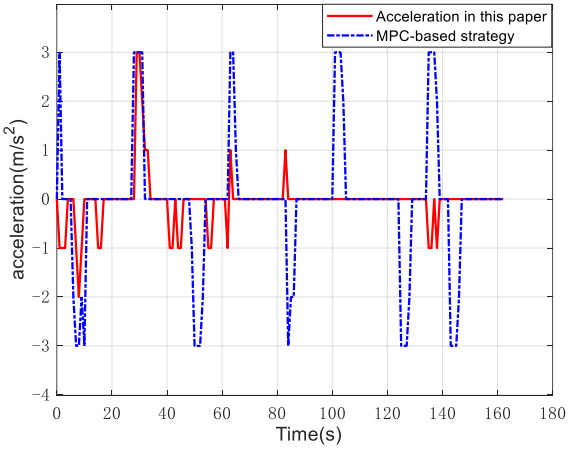

Fig. 5 Acceleration comparison

As can be seen from Fig. 15, both this paper's strategy and the MPC-based strategy realize full green light passing. From Fig. 16, it can be seen that the speed of the MPC-based strategy jumps frequently between 0-72km/h. In this paper's strategy, the speed constraint range is small due to the consideration of the limitation of the traffic density information on the passing sed, so the speed does not have obvious fluctuations, and the highest speed is 54km/h, and the lowest speed is 18km/h. In the same way, the results in Fig. 17 show that the MPC-based strategy has a sharp acceleration/deceleration the number of times is significantly more than the strategy in this paper.

As seen in Fig. 18, the strategy of this paper has a significant advantage in terms of energy consumption. After the vehicle travels 1500 m, the SOC of the MPC-based strategy is reduced by 0.0065, and the SOC of this paper's strategy is reduced by 0.0051, which reduces the SOC consumption by 21.53% compared to the former. This is because the MPC-based strategy, which only utilizes the phase information of the signal lights and ignores the information of traffic density, has a large range of speed fluctuations, and has a large number of sharp accelerations/decelerations, which increases energy loss to some extent. extent increases the energy loss. The strategy in this paper directly aims at

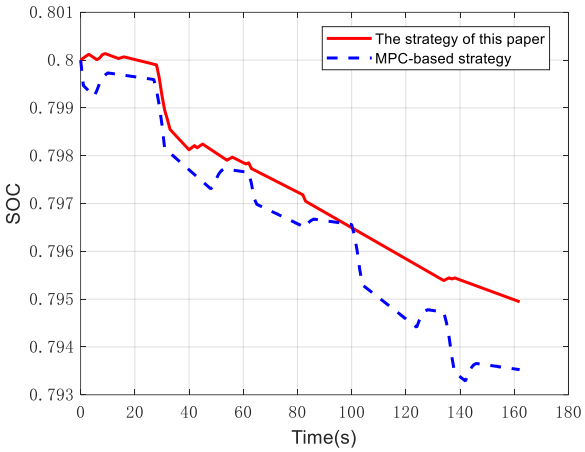

Fig. 6 SOC comparison

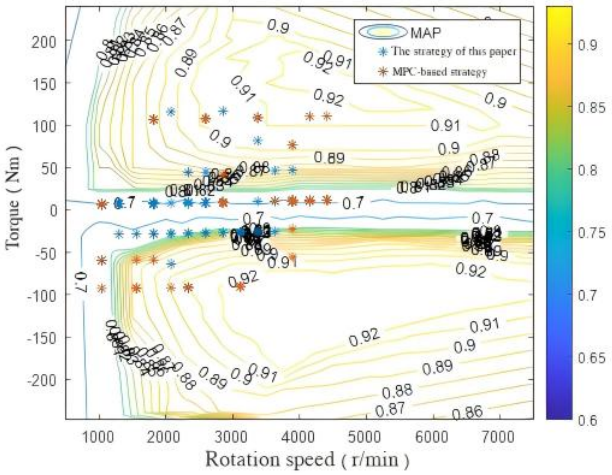

Fig. 7 Comparison of motor operating points

economy and takes into account the effect of traffic flow on the passing speed, with a small range of speed constraints, planning a smoother speed, keeping the uniform speed constant in some periods, and therefore, the SOC change is linear in the corresponding time period. The vehicle energy consumption is greatly reduced by trying to save energy while satisfying the all-green light passage. In addition, from the SOC curve, it can be seen that the SOC curve of the MPC-based strategy shows a rapid decreasing trend, while the SOC curve of this paper's strategy shows a gentle decreasing trend, which further verifies the advantages of this paper's strategy. Fig. 19 shows the distribution of motor operating points for the two strategies, the MPC-based strategy, the distribution of operating points is located in the motor low-efficiency interval, and the motor speed range span; this paper's strategy operating points are centrally distributed, and more distributed in the high-efficiency interval.

The comparison results of the two strategies in terms of ΔSOC, average acceleration absolute value a_{avg}, average velocity a_{avg}, and planning strategy runtime t_{run} are shown in Table 4. In this paper, the strategy battery SOC is reduced by 0.0051, the average acceleration is 0.0429 m/s^2 the power consumption is reduced by 28.76%, and the average acceleration is reduced by 30% compared to the MPC-based strategy. The average speed of both strategies is 9.2883 m/s, which ensures consistent passage time. The difference in runtime between the two strategies is 2.23 s.

Table4

Comparison of different strategies

Speed Planning Strategies	ΔSOC	a_{avg}, m/s^2	v_{avg}, m/s	t_{run}, s
MPC-based strategies	-0.0065	0.0613	9.2883	10.22
The strategy of this paper	-0.0051	0.0429	9.2883	12.45

5.2. Experimental analyses

Intelligent trolley is used as the experimental object, the signal light information and traffic density information are set through the upper computer, and the intelligent trolley runs the algorithm to be verified after accepting the signal light status and the front vehicle status. The trolley control module is a STM32 microcontroller, which accepts the control signal from the trolley calculation module, controls the speed of the trolley in real time, and collects the speed of the trolley in real time and sends it to the trolley calculation module.

The control step of the trolley is 1 s, the sampling interval is 1 s, and the parameters related to the distance in the experiment are scaled down in equal proportions, and the scale γ is as follows:

$$\gamma = \frac{l_{\text{smart carts}}}{l_{\text{actual vehicles}}}, \tag{59}$$

where $l_{smart\ carts}$ is the body length of the intelligent trolley, $l_{actual\ vehicles}$ is the body length of the actual vehicle.

The distance and timing information between signals are shown in Table 5. The total length of the experimental road after equal scaling is 75 m. The starting positionof the trolley is 10 m before the first signal, the initial moment of the trolley movement is after the 10th second of the signal, and the initial speed of the trolley is 0.7 m/s. Traffic density information is set in advance by the host computer, and at the same time, it is pushed to the intelligent trolley in real time. Similarly, two control methods are used for the experiment, and the test process is shown in Fig. 20.

Table 6 shows the data collected in the experimental process of this paper's vehicle speed planning strategy, with a sampling interval of 1 s, including sampling

Table5

Phase information of five signals at the time of the experiment

Junction ids	Junction location, m	Red light timing info, s	Green light timing info, s
1	10	30	40
2	30	30	40
3	45	30	40
4	65	30	40
5	75	20	20

Fig. 20 Experimental scene

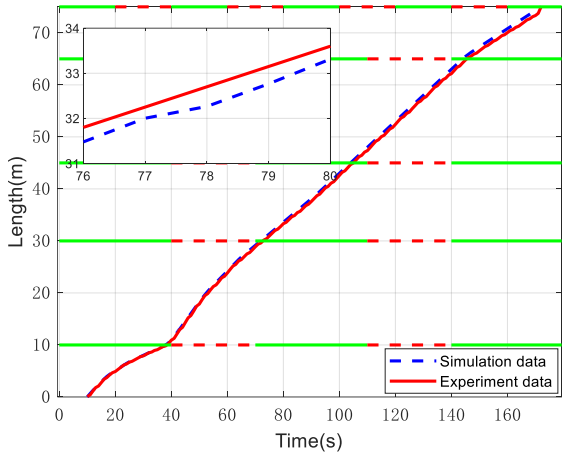

Fig. 21 Displacement curve comparison

Table 6

Experimental data of this paper's strategy

Sampling time, s	Trolley displacement, m	Trolley speed, m/s	Trolley acceleration, m/s^2
0	0	0	0
1	0.0902	0.3810	0.3811
2	0.3843	0.6140	0.2330
3	1.1412	0.5880	–0.0260
…	…	…	…
162	73.7440	0.3480	–0.0100
163	75	0.3480	0.0031

time, vehicle displacement, vehicle speed and vehicle acceleration. The data in Table 6 and the simulation data based on DP-MPC in the previous section are compared and organized, and the experimental results are obtained as shown in Fig. 21, Fig. 22 and Fig. 23. The results show that the strategy in this paper realizes all-green-light passing, a small range of speed fluctuation, and a small number of sharp acceleration/deceleration. However, by comparing with the simulation data, it is found that under the same working conditions, the displacement, speed change and acceleration change of the intelligent trolley have fluctuations and lags to a certain extent, mainly because of the use of wireless communication, the intelligent trolley receives and sends the data with a certain time difference, and also due to the performance of the components of the intelligent trolley and the actual vehicle there is a certain gap.

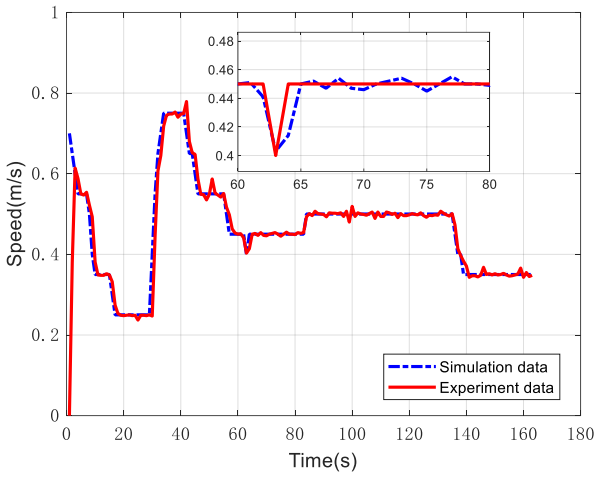

Fig. 22 Velocity profile

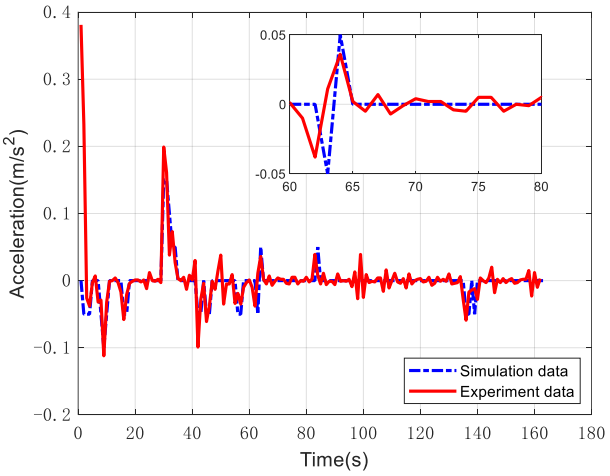

Fig. 8 Comparison of acceleration curves

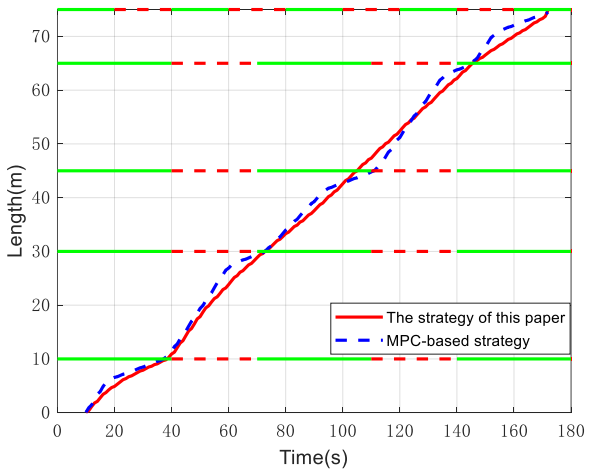

Fig. 9 Comparison of experimental displacements for different speed planning strategies

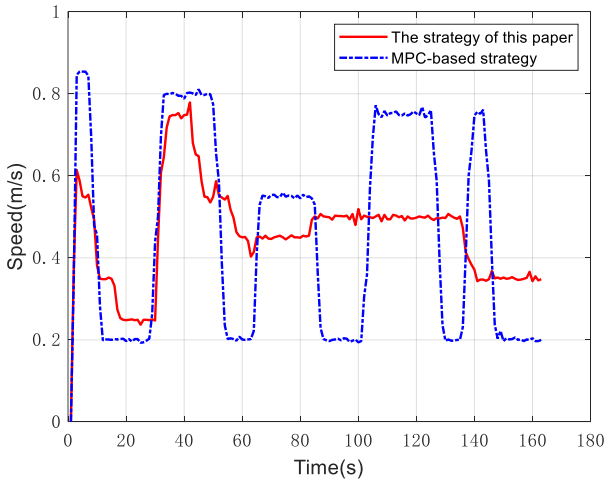

Fig. 10 Comparison of experimental speeds for different speed planning strategies

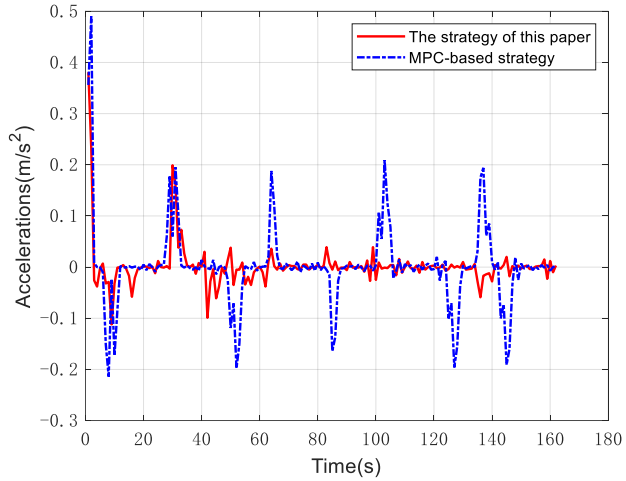

Fig. 11 Comparison of experimental acceleration for different speed planning strategies

Table 7

Comparison of power consumption

Experimental series	Power test value, mAh			Power consumption	
	The strategy of this paper	MPC-based	Total battery capacity	The strategy of this paper	MPC-based
1	5494	5443	5630	136	187
2	5490	5439	5630	140	191
3	5491	5442	5630	139	188
average values	5491.66	5441.33	5630	138.33	188.66

Fig. 24, Fig. 25 and Fig. 26 show the comparison of displacement, vehicle speed and acceleration for the two speed planning strategies, respectively. The results show that the MPC-based strategy can pass all green lights, but the strategy in this paper has less speed fluctuation and fewer sharp accelerations and decelerations of the vehicle, which is very favorable to improve the vehicle economy.

In order to further quantify the superiority of the economic performance of this paper's strategy, the battery power consumption is tested in this paper, and three sets of measurement comparison experiments are conducted, and the experimental results are shown in Table 7. In the three experimental tests, the power consumed by this paper's strategy is smaller than that of the MPC-based strategy, indicating that the economic performance of the strategy proposed in this paper is better, which is consistent with the simulation results.

6. Conclusions

This study proposed an interval-analysis-based vehicle speed optimization method for urban road conditions by jointly considering traffic density information and traffic signal phase information, so as to achieve economical speed planning under continuous signalized intersections.

1. A passing speed interval extraction method based on road passing rules was developed. By incorporating traffic density constraints into the feasible speed interval, the proposed method can better reflect actual urban traffic conditions than conventional methods that mainly rely on SPaT information and speed limits, thereby improving the adaptability of speed planning to dynamic driving environments.

2. An MPC-DP speed planning framework was established with the objective of minimizing vehicle energy consumption. By introducing DP into the MPC prediction horizon, the proposed framework enhances the global optimization capability while maintaining the rolling optimization performance, thus achieving a better balance between economy and real-time applicability.

3. Simulation results showed that the proposed method enabled the vehicle to pass five consecutive signalized intersections with all green lights over a 1500 m road segment. Compared with the MPC-based strategy considering only signal phase information, the proposed method generated a smoother speed trajectory, reduced the SOC drop from 0.0065 to 0.0051, lowered the energy consumption by 21.53%, and decreased the average absolute acceleration from 0.0613 m/s² to 0.0429 m/s².

4. Experimental results further verified the effectiveness of the proposed method. Compared with the MPC strategy, the proposed method exhibited smaller speed fluctuations and lower power consumption, reducing the average power consumption from 188.66 mAh to 138.33 mAh, which demonstrates good energy-saving performance and consistency with the simulation results.

In summary, the main originality of this study lies in introducing interval analysis under traffic-density constraints into urban vehicle speed planning and integrating it with the MPC-DP framework. The results demonstrate that the proposed method can ensure all-green-light passing while effectively reducing vehicle energy consumption and improving the smoothness and practical applicability of speed planning.

Declaration of Conflicting Interests

The author(s) declared no potential conflicts of interest concerning the research, authorship, and/or publication of this article.

Funding

The author(s) disclosed receipt of the following financial support for the research, authorship, and/or publication of this article: This research was supported by the Key Projects of Natural Science Research in Colleges and Universities of Anhui Province (Grant No. 2022AH051050).

References

1. **Ndashimye, E.; Ray, S. K; Sarkar, N. I.; Gutiérrez, J. A.** 2017. Vehicle-to-infrastructure communication over multi-tier heterogeneous networks: A survey, Computer Networks 112: 144-166. https://doi.org/10.1016/j.comnet.2016.11.008.
2. **Asadi, B.; Vahidi, A.** 2009. Predictive Use of Traffic Signal State for Fuel Saving, IFAC Proceedings Volumes 42(15): 484-489. https://doi.org/10.3182/20090902-3-US-2007.0064.
3. **Nie, Z.; Farzaneh, H.** 2022. Real-time dynamic predictive cruise control for enhancing eco-driving of electric vehicles, considering traffic constraints and signal phase and timing (SPaT) information, using artificial-neural-network-based energy consumption model, Energy 241: 122888. https://doi.org/10.1016/j.energy.2021.122888.
4. **Jin, Q.; Wu, G.; Boriboonsomsin, K.; Barth, M. J.** 2016. Power-Based Optimal Longitudinal Control for a Connected Eco-Driving System, IEEE Transactions on Intelligent Transportation Systems 17(10): 2900-2910. https://doi.org/10.1109/TITS.2016.2535439.
5. **Xia, H; Boriboonsomsin, K; Barth, M.** 2013. Dynamic eco-driving for signalized arterial corridors and its indirect network-wide energy/emissions benefits, Journal of Intelligent Transportation Systems 17(1): 31-41. https://doi.org/10.1080/15472450.2012.712494.
6. **HomChaudhuri, B.; Vahidi, A; Pisu, P.** 2017. Fast Model Predictive Control-Based Fuel Efficient Control Strategy for a Group of Connected Vehicles in Urban Road Conditions, IEEE Transactions on Control Systems Technology 25(2): 760-767. https://doi.org/10.1109/TCST.2016.2572603.
7. **Mandava, S; Boriboonsomsin, K; Barth, M.** 2009. Arterial velocity planning based on traffic signal information under light traffic conditions, 12th International IEEE Conference on Intelligent Transportation Systems: 160-166. https://doi.org/10.1109/ITSC.2009.5309519.
8. **HE, C. R.; Maurer, H; Orosz, G.** 2016. Fuel Consumption Optimization of Heavy-Duty Vehicles With Grade, Wind, and Traffic Information, ASME Journal of Computational and Nonlinear Dynamics 11(6): 061011. https://doi.org/10.1115/1.4033895.
9. **De Nunzio, G.; de Wit, C. C.; Moulin, P.; Di Domenico, D.** 2016. Eco-driving in urban traffic networks using traffic signals information, International Journal of Robust and Nonlinear Control 26(6): 1307-1324. https://doi.org/10.1002/rnc.3469.
10. **Luo, Y.; Hu, S.; Zhang, S.** 2017. Multi-segment green light optimal speed advisory for hybrid vehicles, China Journal of Highway and Transport 30: 119-126. https://doi.org/10.19721/j.cnki.1001-7372.2017.10.015.
11. **Xin, Z.; Yu, Z.; Guo, Q.; Lin, Q.; Li, S.; Xu, C.** 2018. Fuel-saving driving strategy for connected vehicles in multiple signalized intersections, Journal of Tsinghua University (Science and Technology) 58(7): 684-692. https://doi.org/10.16511/j.cnki.qhdxxb.2018.22.036.
12. **Liao, G.L.; Zheng, L.; Zhang, Z.D.; Li, Y.N.; Yu, Y.H.** 2022. Optimal speed planning and collision avoidance control for electric vehicles considering traffic lights, Scientia Sinica (Technologica) 52(7): 1134-1144. https://doi.org/10.1360/SST-2021-0133.
13. **Leng, J; Sun, C; Lu, B.** 2021. Fast energy saving speed planning through multi signal intersections of intelligent vehicles, Automotive Engineering 43(10): 1442-1447. https://doi.org/10.19562/j.chinasae.qcgc.2021.10.004.
14. **Zhang, B; Guo, G; Wang, L.Y.; Wang, Q.** 2018. Vehicle speed planning and control for fuel consumption optimization with traffic light state, Acta Automatica Sinica 44(3): 461-470. https://doi.org/10.16383/j.aas.2018.c160684.
15. **Liu, P.; Li, Z.; Jiang, P.; Shu, H.; Liu, Z.** 2022. A new method for vehicle speed planning and model prediction control under V2I, Journal of Chongqing Jiaotong University (Natural Science) 41(7): 27-33. https://doi.org/10.3969/j.issn.1674-0696.2022.07.05.
16. **Chen, H.; Zhuang, W.; Yin, G.; Dong, H.** 2021. Eco-driving control strategy of connected electric vehicle at signalized intersection, Journal of Southeast University/Dongnan Daxue Xuebao (Natural Science Edition) 51(1): 178-186. https://doi.org/10.3969/j.issn.1001-0505.2021.01.024.
17. **Chen, X.; Qian, L.; Wang, Q.** 2024. Eco-driving at signalized intersections under uncertain traffic conditions, Proceedings of the Institution of Mechanical Engineers Part D-Journal of Automobile Engineering 238(2-3): 509-520. https://doi.org/10.1177/09544070221128181.
18. **Dong, H; Zhuang, W; Chen, B; Lu, Y; Liu, S; Xu, L; Pi, D ; Yin, G.** 2022. Predictive energy-efficient driving strategy design of connected electric vehicle among multiple signalized intersections, Transportation Research Part C-Emerging Technologies 137: 103595. https://doi.org/10.1016/j.trc.2022.103595.
19. **Hewing, L.; Wabersich, K. P.; Menner, M; Zeilinger M. N.** 2020. Learning-Based Model Predictive Control: Toward Safe Learning in Control, Annual Review of Control Robotics and Autonomous Systems 3(1): 269-296. https://doi.org/10.1146/annurev-control-090419-075625.
20. **Xie, S.; Hu, X; Xin, Z.; Brighton, J.** 2019. Pontryagin's Minimum Principle based model predictive control of energy management for a plug-in hybrid electric bus, Applied Energy 236(15): 893-905. https://doi.org/10.1016/j.apenergy.2018.12.032.
21. **Qi, S.** 2020. Research on vehicle speed planning algorithm for pure electric vehicles in intelligent and connected scenario, Automobile Applied Technology: 28-30. https://doi.org/10.16638/j.cnki.1671-7988.2020.07.009.

L. Zhu, H. Shi, L. Wang, M. Qiu, H. Zhao

RESEARCH ON OPTIMIZATION METHOD OF VEHICLE SPEED IN URBAN ROAD CONDITIONS BASED ON INTERVAL ANALYSIS

S u m m a r y

Energy saving is the theme of automobile development, and intelligence and networking are the inevitable trend of automobile technology development. Aiming at the influence of traffic information on vehicle energy consumption, an economic speed planning method for intelligent connected vehicles based on interval analysis is proposed. Firstly, based on cellular automata and confidence interval theory, traffic information rules are introduced, and a road speed interval extraction method considering traffic density and traffic signal phase information is established. Secondly, according to the vehicle driving energy consumption model, the objective function of economic speed planning is established, and the traffic speed interval under different driving conditions is taken as the dynamic constraint condition, and the optimal control problem model of vehicle economic speed planning under urban road conditions is established; Then, the optimal control problem of vehicle economic speed is transformed into a model predictive control problem, and the DP algorithm is used to solve the optimal control sequence in each predictive domain, and the optimal speed sequence is planned by cyclic rolling optimization. Finally, through simulation and experimental verification, the results show that the method proposed in this paper can not only achieve all-green traffic at signal intersections, but also achieve good energy-saving effect, and the planning algorithm has fast calculation speed.

Keywords: intelligent connected vehicles, traffic information, traffic speed range, speed planning.

Received March June 12, 2025
Accepted April 24, 2026